Targeting DNA with "light-up" pyrimidine triple-helical forming oligonucleotides conjugated to stabilizing fluorophores (LU-TFOs)

Brice-Loïc Renard, Rémy Lartia† and Ulysse Asseline*

Received 1st August 2008, Accepted 19th August 2008
First published as an Advance Article on the web 16th October 2008
DOI: 10.1039/b813289e

The synthesis of triple-helix-forming oligonucleotides (TFOs) linked to a series of cyanine monomethines has been performed. Eight cyanines including one thiocyanine, four thiazole orange analogues, and three quinocyanines were attached to the 5′-end of 10-mer pyrimidine TFOs. The binding properties of these modified TFOs with their double-stranded DNA target were studied by absorption and steady-state fluorescence spectroscopy. The stability of the triplex structures depended on the cyanine structure and the linker size used to connect both entities. The most efficient cyanines able to stabilize the triplex structures, when attached at the 5′-end of the TFO, have been incorporated at both ends and provided triplex structures with increased stability. Fluorescence studies have shown that for the TFOs involving one cyanine, an important intensity increase (up to 37-fold) in the fluorescent signal was observed upon their hybridization with the double-stranded target, proving hybridization. The conjugates involving thiazole orange attached by the benzothiazole ring provided the most balanced properties in terms of triplex stabilization, fluorescence intensity and fluorescence enhancement upon hybridization with the double-stranded target. In order to test the influence of different parameters such as the TFO sequence and length, thiazole orange was used to label 17-mer TFOs. Hybridizations of these TFOs with different duplexes, designed to study the influence of mismatches at both internal and terminal positions on the triplex structures, confirmed the possibility of triplex formation without loss of specificity together with a strong fluorescence enhancement (up to 13-fold).

Introduction

The detection of specific nucleic acid sequences by the hybridization of fluorescent oligonucleotides is widely used in basic research, diagnostics and biotechnology.[1–6] In the past few years a series of fluorescent oligonucleotides able to produce a fluorescence emission change in the presence of single-stranded target sequences, proving the hybridization, has been reported. However, only a few examples of emission changes in the presence of their double-stranded DNA targets have been described.[7–11] The first concerns pairs of TFOs conjugated to labels designed in such a way as to produce FRET upon hybridization with the double-stranded DNA target.[7] The second involves light-up probes, that is one TFO labelled with one (or two identical) fluorophores, whose fluorescence is enhanced upon triplex formation. They were labelled with either oxazole orange, providing a 3-fold fluorescence enhancement upon hybridization[8] or a ruthenium complex giving a 10-fold increase.[9] Pyrimidine TFOs doubly labelled with perylene have also shown a moderate 3-fold fluorescence enhancement in the presence of the target sequence.[10] Another example of fluorogenic probes able to detect specific sequences on DNA targets are peptide nucleic acid (PNA) molecular beacons.[11] These probes are able to dissociate the double strand to hybridize with their target sequences. During the past decade a great deal of effort has been devoted to modifying TFOs to improve binding properties to their cognate sequences in a cellular environment.[12,13] These developments have led to TFOs able to specifically and strongly hybridize to their double-stranded DNA targets. These TFOs can be used to detect specific sequences on DNA duplexes without having to separate both strands. We now report the synthesis and photophysical properties of pyrimidine TFOs labelled with monomethine cyanines. The influence of the labelling on the triplex stability was studied by thermal denaturation followed by absorption spectroscopy. The changes in the fluorescence emission, upon triplex formation, were evaluated by steady-state fluorescence experiments. We have also investigated the possibility of increasing the difference in the fluorescence emission between the free and the hybridized labelled TFO by quenching the fluorescence of the free TFOs by hybridization with a complementary short probe involving a quencher. The influence of different parameters such as the TFO sequence and length and the presence of mismatches at both the internal and terminal positions on the triplex structures have also been studied. The possibility of forming a triplex with increased stability by using a labelled TFO designed to hybridize with a duplex involving a pyrimidine–purine base-pair inversion has also been investigated.

Centre de Biophysique Moléculaire, CNRS UPR 4301, affiliated with the University of Orléans and INSERM, Rue Charles Sadron, 45071 Orléans Cedex 02, France. E-mail: asseline@cnrs-orleans.fr; Fax: + 33-2-38-63-15-17

† Present address: Département de Chimie Moléculaire, UMR 5250, ICMG FR 2607, CNRS, Université Joseph Fourier, BP 53, 38041 Grenoble Cedex 9, France

Results and discussion

Structures and experimental design

These fluorescent TFOs are made of an oligopyrimidine sequence involving either one monomethine cyanine attached at the 5′-end or two (identical ones) linked to both ends. Their structures are shown in Fig. 1. The eight monomethine cyanines, including one thiocyanine (**Th**), four thiazole orange analogues (**2TO**, **4TO**, **2TO′**and **4TO′**), and three quinocyanines (**22′Q**, **24′Q** and **42′Q**), used as the labels were previously prepared[14] but were not used to label TFOs. Monomethine cyanines were chosen because they are able to intercalate into double-stranded nucleic acid targets. Thus, reduction of the rotation around the methine bond, provided by intercalation, has been reported to be one of the parameters responsible for a strong increase in fluorescence observed on binding of the most frequently used monomethine cyanine, thiazole orange, with DNA duplexes.[15–18] They were, firstly, covalently linked to the 5′-end of a 10-mer oligopyrimidine sequence d-$^{5'}$TTTTCTTTTC$^{3'}$ *via* a phosphothiolodiester bond and an octamethylene linker (Fig. 1). This sequence was chosen because it had been used previously in our laboratory for the development of intercalator–TFO conjugates.[19,20] The pyrimidine DNA sequences were reported to hybridize with their duplex DNA targets in a parallel orientation with respect to the purine strand.[12,21–22] Labelling was first performed at the 5′- position because the duplex–triplex junction at the 5′-end of the triplex nucleic acid structure is favourable for intercalation.[21–23] We chose linkers with eight methylene groups because it has been shown that linkers with lengths equal or superior to five or six carbon atoms are required to enable intercalation.[22,24,25]

To study the influence of the linker size used to connect the TFO and the fluorophore, the most efficient cyanine at stabilizing the triplex structure, **4TO′**, was also linked to the 5′- end of the TFO *via* linkers involving seven, six, five and four methylene groups.[26] Bis-conjugations at both the 5′- and 3′-ends of the TFO of the most efficient cyanines at stabilizing the triplex structure when attached to the 5′-end of the TFO, **4TO′** and **2TO**, were also performed using the linker size (eight methylene groups) showing the strongest stability when **4TO′** was attached to the 5′-end. Bis-labelling was also achieved with quinocyanine **24′Q** giving the greatest fluorescence increase upon triplex formation. The linker size used to connect **4TO′** to the 3′-end was also increased by three

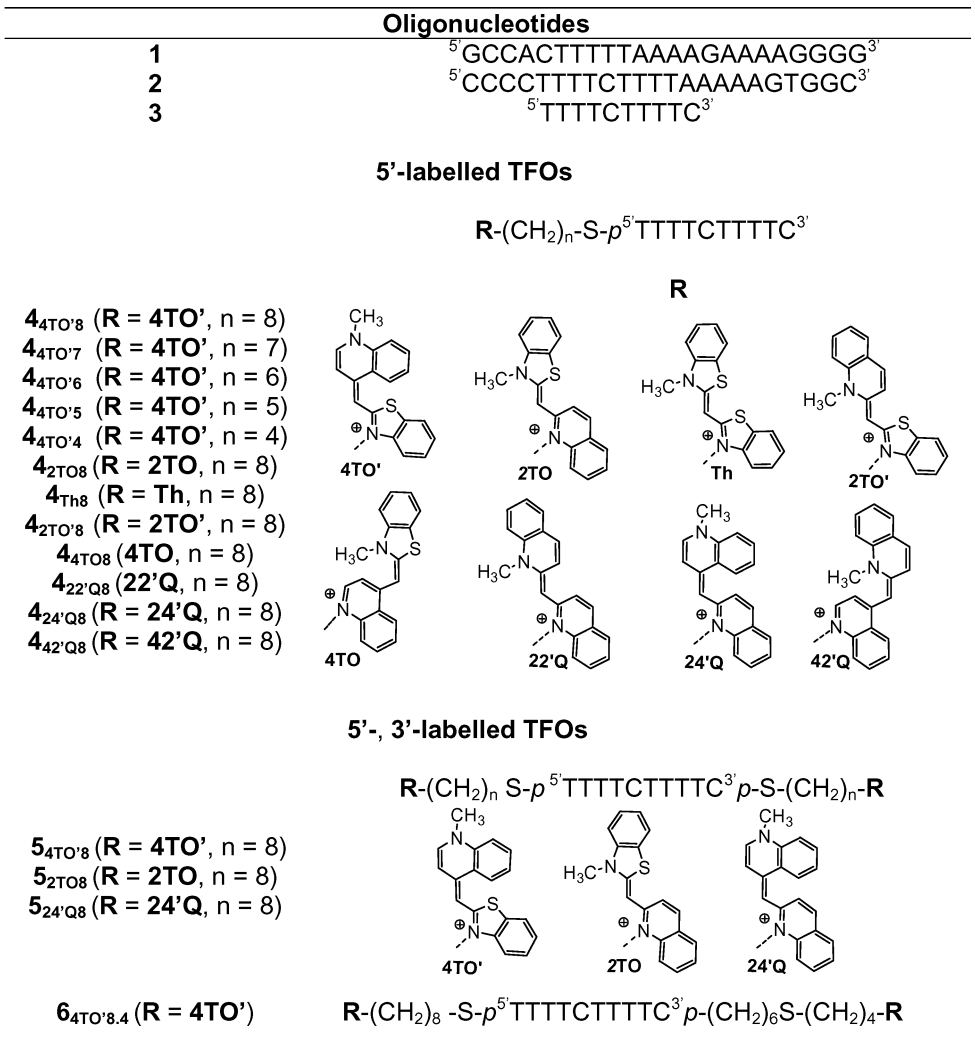

Fig. 1 Structures of labelled TFOs and oligonucleotides.

atoms because it has been demonstrated that the stabilization of triple helices by an acridine derivative attached to the 3′-end of a TFO required the use of a longer linker as compared with the size of the one used to link this intercalator at the 5′-position.[27] We report here the synthesis of these TFO-conjugates and their binding properties with their double-stranded DNA targets, evaluated by absorption and fluorescence spectroscopy.

Synthesis

The attachment of labels to oligonucleotides can be achieved following two strategies.[28] The first consists in their direct incorporation using the phosphoramidites of the labels (or the phosphoramidite derivatives of modified nucleosides bearing the labels). The 3′-modification can also be achieved by using modified supports involving these labels. However, the direct incorporation of labels during the oligonucleotide synthesis requires labels or nucleoside analogues able to withstand the chemical conditions needed for the deprotection step and that are soluble in organic solvents. Another strategy consists in the post-synthetic attachment of labels to various positions of the oligonucleotides by specific reactions between convenient functional groups incorporated at pre-selected positions on both entities. Since our previous work has shown that cyanines are not very stable in strong alkali conditions (unpublished results), we chose the post-synthetic coupling strategy for the preparation of the labelled TFOs (*vide infra*).

Synthesis of modified TFOs bearing the cyanines at their 5′-ends. Synthesis of conjugates involving cyanines linked to the 5′-end of the TFO $\mathbf{4}_{4TO'8}$ to $\mathbf{4}_{42'Q8}$ relies on the incorporation of a thiophosphate group at the 5′-end of the oligonucleotide bound to the support **7** (Scheme 1a). The TFO was synthesized by phosphoramidite chemistry[29] and after an additional detritylation step, a masked thiophosphate group was added using our previously reported method.[30] After the deprotection step, the crude 5′-thiophosphorylated TFO **4** was reacted with the halogenoalkyl groups of the cyanines, obtained as previously described[14,26] in a mixture of an aqueous bicarbonate buffer and dimethylformamide (see Fig. 1 for the structures). The conjugates were purified by reversed-phase chromatography (see Fig. 2 and Table 1) and characterized by electrospray mass spectrometry (Table 1) and UV–visible analyses (see Table 1 for λ_{max} absorption in the UV and visible range). The visible absorption bands of the different conjugates span from 427 to 561 nm. The UV–visible spectra of the 5′-labelled TFOs $\mathbf{4}_{24'Q8}$, $\mathbf{4}_{2TO8}$ and $\mathbf{4}_{4TO'8}$ are shown in Fig. 3.

Synthesis of TFOs bearing cyanines at both the 5′- and 3′-ends. The synthesis of the bis-conjugated TFOs $\mathbf{5}_{2TO8}$, $\mathbf{5}_{24'Q8}$ and $\mathbf{5}_{4TO'8}$ involving both cyanines attached *via* the same linker length was performed by incorporation of a thiophosphate group at both ends of the TFO (Scheme 1b). The synthesis was performed on our previously reported support **8**.[31] A masked thiophosphate group was then incorporated at the 5′-end as described above. After the deprotection and purification steps, the bis 5′-,3′-thiophosphorylated TFO **5** was reacted with the selected iodoalkylated cyanines to give TFO conjugates $\mathbf{5}_{2TO8}$, $\mathbf{5}_{24'Q8}$ and $\mathbf{5}_{4TO'8}$. The synthesis of the bis-conjugated TFO involving two cyanines attached with linkers of different sizes $\mathbf{6}_{4TO'8.4}$ was performed by incorporation of a thiophosphate group at its 5′-end and a thiol masked function at its 3′-end in order to perform a sequential coupling at each end (Scheme 2). The incorporation of the thiol function at the 3′-end of the TFO was achieved by using a new modified support leading, after the deprotection step, to oligonucleotides with a 6,6′-dithiodihexanol linker.

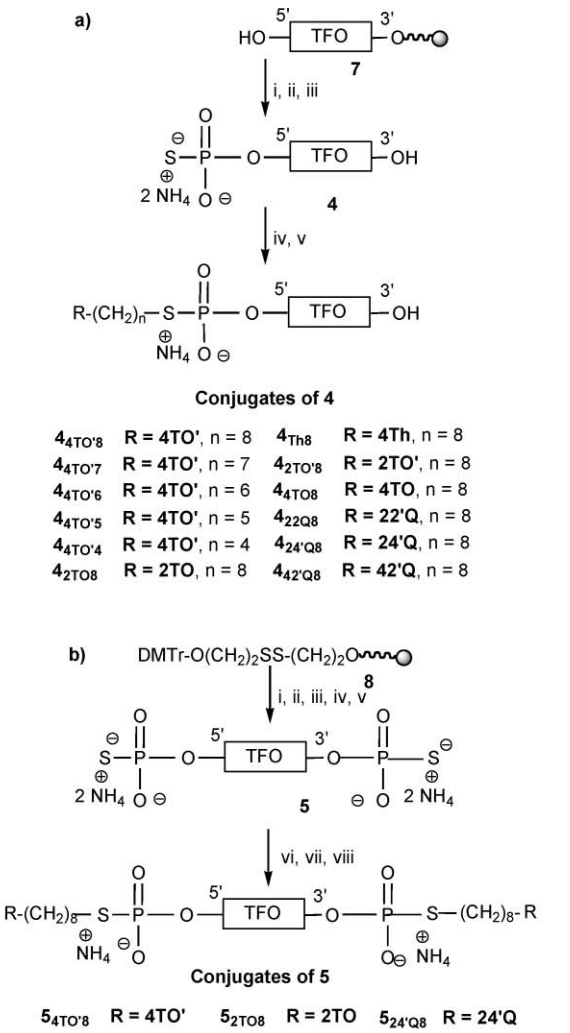

Reagents and conditions:
(a) i: $DMTrOCH_2CH_2SSCH_2CH_2$-O-P(O)(H)(O^-) $HNEt_3^+$, Pivaloyl chloride; ii: CS_2/C_5H_5N; iii: NH_4OH, overnight, 55°C; iv: R-$(CH_2)_n$-I (for R see Figure 1) 2.5% aqueous bicarbonate buffer (pH 9)/ DMF, 6 h at rt; v: purification.
(b) i: H^+; ii: TFO synthesis, H^+; iii: $DMTrOCH_2CH_2SSCH_2CH_2$-O-P(O)(H)(O^-) $HNEt_3^+$, Pivaloyl chloride; iv: CS_2/C_5H_5N; v: NH_4OH + DTT overnight, 55°C; vi: purification; vii: R$(CH_2)_8$I (R = **4TO'**, **2TO** or **24'Q**) 2.5% aqueous bicarbonate buffer (pH 9)/ DMF, 6 h at rt viii: purification.

Scheme 1 Synthesis of 5′-labelled TFOs $\mathbf{4}_{4TO'8}$ to $\mathbf{4}_{42'Q8}$ (a) and 5′-,3′-bis-labelled TFOs $\mathbf{5}_{4TO'8}$, $\mathbf{5}_{2TO8}$ and $\mathbf{5}_{24'Q8}$ (b).

The new support (Scheme 2) was obtained following a five-step procedure. First, thiohexanol **9** was dimerized into 6,6′-dithiodihexanol. The latter was monodimethoxytritylated to give **10**. Then reaction with succinic anhydride followed by coupling with *p*-nitrophenol in the presence of *N*,*N*′-carbodiimide led to the activated ester. The latter was then reacted with aminopropyl controlled pore glass to give the modified support **11** with a loading of 36 μmol g^{-1}. The coupling of the bis-modified TFO **6** with

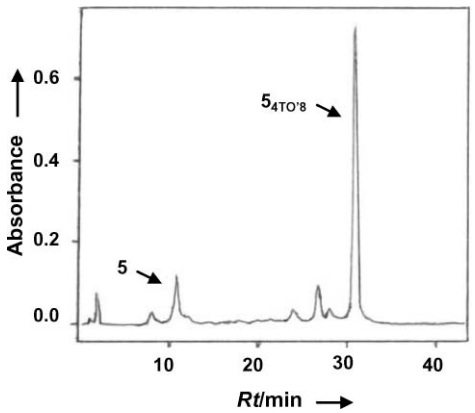

Fig. 2 Reversed-phase HPLC analysis of the coupling reaction between TFO **5** and the cyanine-linker derivative **4TO′**-$(CH_2)_8$I performed on a LiChrospher RP 18 (5 μm) column (125 mm × 4 mm) from Merck using a linear gradient of CH_3CN (5 to 38.5% over 45 min) in 0.1 M aqueous ammonium acetate, pH = 7, with a flow rate of 1 cm^3 min^{-1}. Detection $\lambda = 260$ nm.

4TO′-$(CH_2)_8$-I followed by release of the thiol function by cleavage of the disulfide bridge by treatment with a reducing agent,[32] and reaction with **4TO′**-$(CH_2)_4$-I led to the bis-derivatized $\mathbf{6}_{4TO'8.4}$ involving two TO′ attached *via* linkers of different sizes. Purification of the TFO conjugates was performed by reversed-phase chromatography. The retention times (Table 1) for the conjugates involving two cyanines were higher than those involving only one cyanine. These results indicate the formation of more lipophilic compounds. The UV–visible spectra of the bis-labelled TFOs $\mathbf{5}_{2TO8}$, $\mathbf{5}_{24'Q8}$ and $\mathbf{5}_{4TO'8}$ are shown in Fig. 3.

Absorption studies

Free TFO conjugates. The UV–visible spectra of the TFO-labelled conjugates were recorded between $\lambda = 230$ nm and $\lambda = 700$ nm. The spectra of the 5′-conjugated TFOs contained two main absorption bands. The absorption band in the UV range corresponded to the absorbance of the TFO and the cyanines with a λ_{UV} ~267 nm for all conjugates. The second absorption band in the visible region between $\lambda = 350$ nm and $\lambda = 700$ nm corresponds to the cyanine. The general shape involves a main band with a shoulder at a shorter wavelength. The λ_{max} values in the visible range and the intensity ratios of the UV–visible bands depend on the cyanine considered (data not shown). A comparison of the UV–visible spectra of the mono- and bis-labelled TFOs, involving **2TO**, **24′Q** and **4TO′** as the labels, shows different shapes in the visible range (Fig. 3).

Conjugate $\mathbf{5}_{4TO'8}$ exhibited a main band in the visible range at $\lambda = 478$ nm and a shoulder at $\lambda = 508$ nm with the one at

Table 1 Characterization of conjugates and T_m data

ODNs	Reversed-phase R_t [a]	Mass analysis [b]		E/M^{-1} cm^{-1} [c]			
		Calculated	Found	λ_{max} UV	λ_{max} vis	T_m/°C (±0.5 °C)[d]	ΔT_m/°C (±1 °C)
4	11 min 37 sec	$C_{98}H_{128}N_{22}O_{68}P_{10}S = 3044.00$	3044.06	80 100 (267)	—	—	—
$\mathbf{4}_{4TO'8}$	28 min 49 sec	$C_{124}H_{158}N_{24}O_{68}P_{10}S_2 = 3446.60$	3446.37	116 500 (267)	82 700 (508)	37.5	+24.5
$\mathbf{4}_{4TO'7}$	26 min 27 sec	$C_{123}H_{156}N_{24}O_{68}P_{10}S_2 = 3432.57$	3431.63	116 500 (267)	82 700 (508)	35.0	+22.0
$\mathbf{4}_{4TO'6}$	24 min 05 sec	$C_{122}H_{154}N_{24}O_{68}P_{10}S_2 = 3418.54$	3417.55	116 500 (267)	82 700 (508)	32.5	+19.5
$\mathbf{4}_{4TO'5}$	22 min 28 sec	$C_{121}H_{152}N_{24}O_{68}P_{10}S_2 = 3404.52$	3403.64	116 500 (267)	82 700 (508)	29.0	+16.0
$\mathbf{4}_{4TO'4}$	22 min 21 sec	$C_{120}H_{150}N_{24}O_{68}P_{10}S_2 = 3390.49$	3389.88	116 500 (267)	82 700 (508)	26.5	+13.5
$\mathbf{4}_{2TO8}$	28 min 42 sec	$C_{124}H_{158}N_{24}O_{68}P_{10}S_2 = 3446.60$	3446.39	120 300 (267)	62 700 (488)	32.5	+19.5
$\mathbf{4}_{Th8}$	28 min 19 sec	$C_{122}H_{156}N_{24}O_{68}P_{10}S_3 = 3452.62$	3452.23	95 600 (267)	77 100 (427)	31.0	+18.0
$\mathbf{4}_{2TO'8}$	28 min 36 sec	$C_{124}H_{158}N_{24}O_{68}P_{10}S_2 = 3446.60$	3446.01	93 500 (267)	48 400 (486)	28.0	+15.0
$\mathbf{4}_{4TO8}$	28 min 29 sec	$C_{124}H_{158}N_{24}O_{68}P_{10}S_2 = 3446.60$	3446.27	89 600 (267)	65 300 (508)	27.5	+14.5
$\mathbf{4}_{22'Q8}$	28 min 20 sec	$C_{126}H_{160}N_{24}O_{68}P_{10}S = 3440.57$	3440.05	82 600 (267)	58 600 (526)	26.5	+13.5
$\mathbf{4}_{24'Q8}$	28 min 51 sec	$C_{126}H_{160}N_{24}O_{68}P_{10}S = 3440.57$	3440.00	83 600 (267)	59 200 (561)	25.5	+12.5
$\mathbf{4}_{42'Q8}$	28 min 32 sec	$C_{126}H_{160}N_{24}O_{68}P_{10}S = 3440.57$	3439.81	82 400 (267)	42 100 (560)	19.5	+6.5
5	11 min 48 sec	$C_{98}H_{128}N_{22}O_{68}P_{10}S = 3139.03$	3141.54	80 100 (267)	—	—	—
$\mathbf{5}_{4TO'8}$	32 min 47 sec	$C_{150}H_{188}N_{26}O_{70}P_{11}S_4 = 3944.24$	3942.79	145 000 (267)	143 600 (478)	45.0	+32.0
$\mathbf{5}_{2TO8}$	34 min 27 sec	$C_{150}H_{188}N_{26}O_{70}P_{11}S_4 = 3944.24$	3943.36	154 500 (267)	143 900 (459)	39.0	+26.0
$\mathbf{5}_{24'Q8}$	32 min 58 sec	$C_{154}H_{192}N_{26}O_{70}P_{11}S_2 = 3932.19$	3931.59	85 800 (267)	74 500 (519)	30.5	+17.5
6	11 min 24 sec	$C_{110}H_{153}N_{22}O_{72}P_{11}S_3 = 3372.43$	3374.41	80 100 (267)	—	—	—
$\mathbf{6}_{4TO'8.4}$	32 min 13 sec	$C_{152}H_{192}N_{26}O_{71}P_{11}S_4 = 3988.30$	4002.41	145 000 (267)	111 500 (479)	43.0	+30.0
$\mathbf{12}_{dab}$	25 min 50 sec	$C_{121}H_{148}N_{54}O_{54}P_{10} = 3530.58$	3530.58	125 500 (256)	29 300 (477)	—	—
$\mathbf{13}_{dab}$	27 min 18 sec	$C_{101}H_{124}N_{44}O_{43}P_8 = 2889.15$	2888.89	103 700 (256)	29 300 (477)	—	—
$\mathbf{14}_{dab}$	27 min 30 sec	$C_{91}H_{112}N_{39}O_{38}P_7 = 2575.94$	2575.95	91 700 (256)	29 300 (477)	—	—
$\mathbf{15}_{dab}$	28 min 12 sec	$C_{81}H_{100}N_{34}O_{33}P_6 = 2262.73$	2263.10	79 700 (256)	29 300 (477)	—	—
$\mathbf{16}_{4TO'8}$	24 min 08 sec	$C_{191}H_{247}N_{41}O_{114}P_{17}S_2 = 5531.93$	5532.59	169 800 (267)	82 700 (508)	See Table 3	
$\mathbf{17}_{4TO'8}$	23 min 24 sec	$C_{191}H_{246}N_{44}O_{113}P_{17}S_2 = 5556.95$	5557.11	172 400 (267)	82 700 (508)	See Table 3	

[a] Retention times obtained by reversed-phase HPLC analyses for the ODNs performed on a LiChrospher RP 18 (5 μm) column (125 mm × 4 mm) from Merck using a linear gradient of CH_3CN (5% to 38.5% over 45 min) in 0.1 M aqueous ammonium acetate, pH 7, with a flow rate of 1 cm^3 min^{-1}. [b] Mass analysis data for the modified TFOs and their conjugates and dabcyl conjugates. [c] Molar absorption coefficients for the modified TFOs and their conjugates (the values in the brackets indicate the corresponding wavelength). For 5′-labelled TFOs **4**, **16** and **17** the ε values at $\lambda = 260$ nm were the approximate sum of the ε values of the TFOs and labels.[14] *E* values were determined experimentally for labelled TFOs **5** and **6**. The same ε values were used for the conjugates involving the same sequence and different linker lengths to connect the label and the TFO. [d] T_m values for triplexes formed by the labelled TFOs and the double-stranded target (**1** + **2**) in a 10 mM sodium phosphate, pH 6, buffer containing 140 mM KCl and 5 mM $MgCl_2$. Concentrations were 1 μM in the duplex target and TFOs. Under the same experimental conditions, the T_m value for the unmodified triplex (**1** + **2** + **3**) was 13 °C.

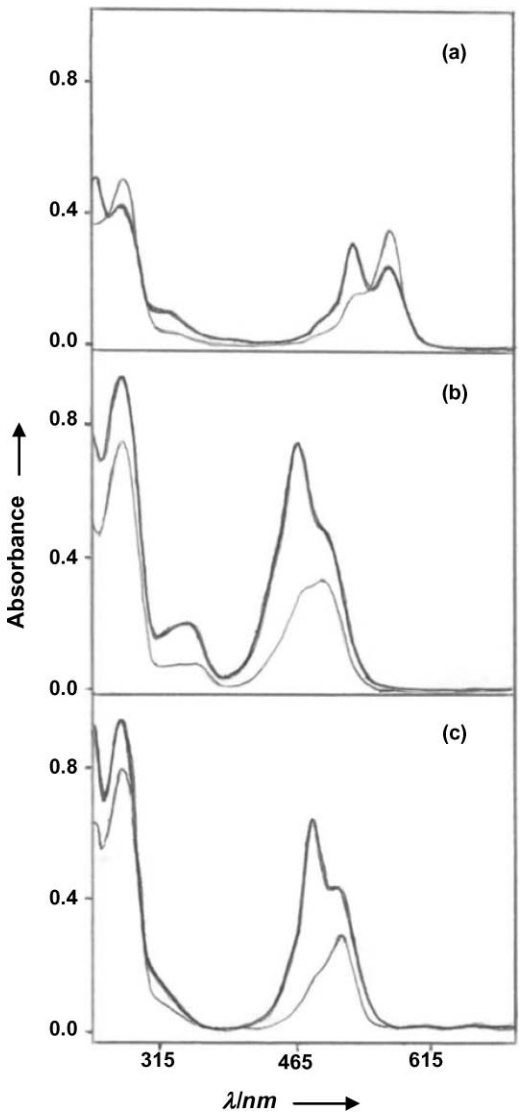

Fig. 3 UV–visible absorption spectra of water solutions of the mono-labelled TFOs (full line) $\mathbf{4}_{24'Q8}$ (a) $\mathbf{4}_{2TO8}$ (b) and $\mathbf{4}_{4TO'8}$ (c); and bis-labelled TFOs (bold line) $\mathbf{5}_{24'Q8}$ (a), $\mathbf{5}_{2TO8}$ (b) and $\mathbf{5}_{4TO'8}$ (c) recorded between $\lambda = 230$ and $\lambda_{\sim} = 700$ nm.

$\lambda = 478$ nm being the more intense, while for the corresponding conjugate $\mathbf{4}_{4TO'8}$ involving only one TO′ residue, the absorption at 478 nm appeared only as a shoulder and the main band was detected at $\lambda = 508$ nm. Upon a temperature increase, from 20 to 60 °C, a blue-shift of 3 nm was observed for the visible band with a slight hypochromism, 2–3%, for the 5′-mono-conjugated TFO $\mathbf{4}_{4TO'8}$ while only hypochromism (4% at 478 nm) was detected for the corresponding bis-conjugated TFO $\mathbf{5}_{4TO'8}$. Similar intensity changes were observed for TFOs $\mathbf{4}_{2TO8}$ and $\mathbf{5}_{2TO8}$ labelled with the **2TO**. The spectrum of the mono-labelled TFO $\mathbf{4}_{2TO8}$ showed a main peak with $\lambda = 488$ nm and a shoulder at $\lambda = 470$ nm, while that of the bis-labelled TFO $\mathbf{5}_{2TO8}$ exhibited a main peak at $\lambda = 459$ nm and a shoulder at $\lambda = 500$ nm. When **24′Q** was used to label the TFO the visible band of the mono-labelled TFO showed a main band at $\lambda = 561$ nm with a shoulder at $\lambda = 528$ nm. The visible spectra of the corresponding bis-labelled TFO exhibited two main bands at $\lambda = 519$ nm and $\lambda = 560$ nm. In addition to the shape difference observed for the visible spectra of mono- and bis-labelled TFOs, the observation of the UV–visible absorption ratio indicated that the absorbance intensities in the visible range for the bis-labelled TFOs were not twice those of the corresponding mono-labelled TFOs. The shift of the visible absorption band to the shortest wavelength observed for the bis-conjugated TFO indicated aggregation of the cyanine dyes. Similar spectrum changes have been previously reported for the thiazole orange dimer.[16] It is likely that, even at 60 °C, due to the flexibility of the oligonucleotide chain, contacts between the two labels were possible.

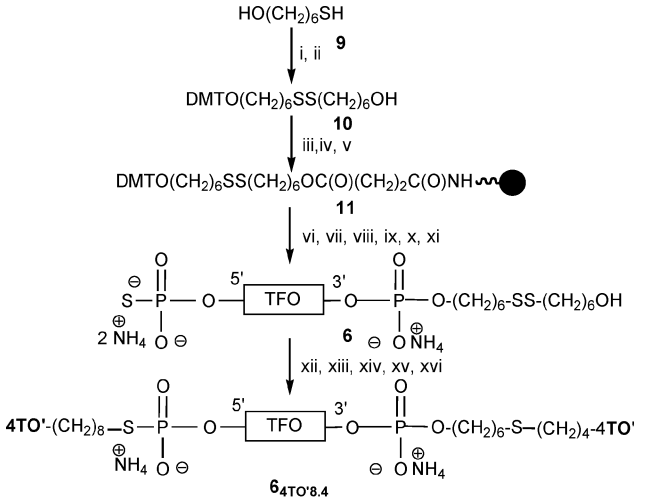

Reagents and conditions:
i:EtOH/NH_4OH, air; ii: DMtrCl/Py; iii: succinic anhydride, 4-dimethylaminopyridine, pyridine; iv: p-nitrophenol, pyridine, dicyclohexylcarbodiimide, dioxane; v: aminopropyl-CPG-500, NEt_3, DMF; vi: H^+; vii: TFO synthesis, H^+; viii: $DMTrOCH_2CH_2SSCH_2CH_2$-O-P(O)(H)(O^-) $HNEt_3^+$, Pivaloyl chloride; ix: CS_2/C_5H_5N; x: NH_4OH overnight, 55°C; xi: purification; xii: **4TO'**-$(CH_2)_8$-I, 2.5 % aqueous bicarbonate buffer (pH 9)/ DMF, 6 h at rt; xiii: purification; xiv: 2.5 % aqueous bicarbonate buffer (pH 9)/TCEP; xv: **4TO'**-$(CH_2)_4$-I/DMF, 6 h at rt; xvi: purification

Scheme 2 Synthesis of the bis-labelled TFO $\mathbf{6}_{4TO'8.4}$

Molar absorption coefficient determination. The molar absorption coefficients (ε_{260nm} values) for the conjugates derived from TFO **4** were estimated to be the sum of the ε values of the TFO and cyanines deducted from ref. 14 (see Table 1). The same ε_{260nm} values were used for the series of conjugates $\mathbf{4}_{4TO'n}$ involving different linker sizes (n = 4, 5, 6, 7 and 8). Because the UV–visible absorption ratio observed for the bis-conjugated TFOs $\mathbf{5}_{4TO'8}$, $\mathbf{5}_{2TO8}$ and $\mathbf{5}_{24'Q8}$ indicated intensities not simply twice those of the corresponding mono-labelled TFOs, their extinction coefficients at 260 nm were determined by titrations of the conjugate solutions in a 10 mM KH_2PO_4 buffer (pH 6), containing 140 mM KCl and 5 mM $MgCl_2$ performed at 3 °C, with solutions of the single-stranded complementary sequence $^{5'}$GGGAAAAGAAAATTT$^{3'}$.[19] The molar extinction coefficient at 260 nm used for $\mathbf{6}_{4TO'8.4}$ was the same as for $\mathbf{5}_{4TO'8}$.

Hybridized TFO-conjugates. Mixing of the mono-conjugated TFO derived from **4** with the double-stranded DNA target **1** + **2** at 3 °C induced only weak spectral modifications that were reversed upon a temperature increase to 65°. These changes showed a

slight red-shift (~4 nm) of the visible absorption band and a weak hyperchromism (4%) (data not shown). In the case of conjugate $\mathbf{5}_{\mathbf{4TO'8}}$ involving two cyanines attached through octamethylene linkers, more important changes were observed resulting in a decrease (24%) in the intensity of the band at 478 nm and an increase (34%) at 508 nm. For conjugate $\mathbf{6}_{\mathbf{4TO'8.4}}$ involving two **4TO′** attached *via* linkers of different sizes, hybridization with the double-stranded target **1** + **2** resulted in similar changes except that the intensities were 18% hyprochromism at 481 nm and 20% hyperchromism at 511 nm. Similar trends were also observed upon hybridization of TFO $\mathbf{5}_{\mathbf{2TO8}}$, resulting in a slight red shift (458 to 465 nm) with 13% hypochromism, and of TFO $\mathbf{5}_{\mathbf{24'Q8}}$, giving a smaller red-shift (490 to 494 nm) with 20% hyperchromism. These changes indicate that in the presence of the duplex, the interactions between the two cyanine units are suppressed. Since a DNA triplex is more rigid than a single-stranded sequence, it is likely that upon hybridization of the conjugates of TFOs **4**, **5** and **6** with the double-stranded target the cyanines are able to interact with only the end of the triplex and a few bases on the overhanging double-stranded target adjacent to the triplex on the side of the cyanine attachment.

Thermal denaturation studies. Experiments were carried out by absorption spectroscopy. Triplex stabilities were determined by thermal denaturation using a 1 : 1 mixture of the conjugates and double-stranded target **1** + **2**. The corresponding unmodified TFO **3** was used as a reference. Two transitions were observed in the melting of each triplex (Fig. 4). The transition with the higher T_m corresponds to the melting of the target duplex (around 62 °C for all complexes) and the transitions with lower T_m to the dissociation of the third strand. The T_m values, listed in Table 1, indicate that the triplex structures formed between the conjugates derived from TFOs **4–6** and the duplex **1** + **2** target were stabilized in all cases as compared to the corresponding complexes formed with the unmodified TFO **3** used as a reference.

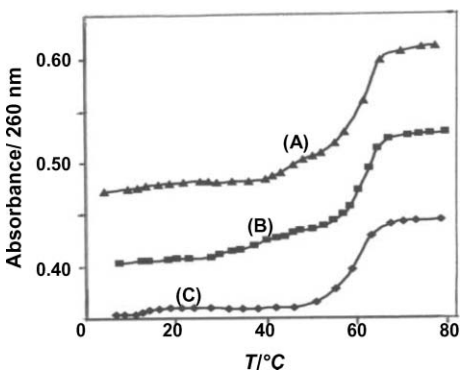

Fig. 4 UV melting profiles (recorded at λ = 260 nm) of the triplex structures formed by conjugates $\mathbf{4}_{\mathbf{4TO'8}}$ (A) and $\mathbf{5}_{\mathbf{4TO'8}}$ (B) and the unmodified TFO **3** (C) in the presence of the duplex target (**1** + **2**). Concentrations were 1 μM in the duplex and in the TFO, in a 10 mM sodium phosphate, pH 6, buffer containing 140 mM KCl and 5 mM $MgCl_2$.

TFOs involving one label at the 5′-end. Different stabilizations were observed depending on the cyanine structures and the linker sizes. A comparison of the stabilization afforded by the cyanines attached *via* the same linker involving eight methylene groups indicated that the most efficient stabilizing group was **4TO′8** (ΔT_m = +24.5 °C) followed by **2TO8** (ΔT_m = +19.5 °C), **Th8** (ΔT_m = +18 °C), **2TO′8** (ΔT_m = +15 °C), **4TO8** (ΔT_m = +14 °C) and the four quinocyanines provided stabilizations ranging from ΔT_m = +6.5 °C to ΔT_m = +13.5 °C. Since it has previously been shown that the attachment of intercalating groups at the 5′-end of TFOs *via* linkers involving five or six methylene groups corresponds to the optimal size for the greatest stability, we chose to attach the most efficient cyanine **4TO′** *via* linkers of decreasing lengths involving seven to four methylene groups. T_m measurements indicated that the stability depended on the linker size and decreased with the length of the linker. The ΔT_m was approximately 3 °C per methylene group. TFO conjugates involving one label attached to the 5′-end *via* an eight-methylene linker form the most stable triplex structures.

*Bis-labelled TFOs **5** and **6**.* In all cases the presence of a second cyanine (conjugates $\mathbf{5}_{\mathbf{4TO'8}}$, $\mathbf{5}_{\mathbf{2TO8}}$, $\mathbf{5}_{\mathbf{24'Q8}}$ and $\mathbf{6}_{\mathbf{4TO'8.4}}$) induced an increase in the stabilization of the triplex as compared with that obtained with the mono-conjugated TFOs. UV melting profiles corresponding to the third strand dissociation of the triplex formed by TFOs $\mathbf{5}_{\mathbf{4TO'8}}$ and $\mathbf{4}_{\mathbf{4TO'8}}$ and by the unmodified TFO **3** are shown in Fig. 4. Stability depended on both the cyanine and the linker length used to attach the second cyanine to the 3′-end. The strongest stabilization (ΔT_m = +32 °C) was observed with $\mathbf{5}_{\mathbf{4TO'8}}$ involving two thiazole orange labels attached *via* a linker of the same length corresponding to the eight methylene groups. An increase in the linker length to attach the cyanine to the 3′-end of the TFO $\mathbf{6}_{\mathbf{4TO'8.4}}$ led to a slight decrease of the triplex stability (ΔT_m = +30 °C). This result is different from the one observed with the TFO labelled with an acridine derivative at both the 5′- and 3′-ends.[27] The presence of the second intercalator **4TO8**, **2TO8** or **24′Q8** led to similar stability increases (ΔT_m = +7.5 °C, ΔT_m = +6.5 °C, and ΔT_m = +5 °C respectively). This increase in the stability of the triple-stranded structures provided by the presence of a second intercalator was also previously reported for TFO–naphthalene[33] and TFO–perylene conjugates.[10]

Fluorescence studies

Fluorescence emission spectra of the conjugates were compared with those of the triplexes. Experiments were performed under the same conditions (concentration, buffer) as for the T_m measurements (see Experimental Section and Table 2). The λ_{exc} and λ_{em} depended on the cyanine (Table 2). Upon hybridization with the double-stranded target **1** + **2**, the λ_{em} did not change as compared with those observed for the free conjugates. The main changes concerned the intensity of the fluorescence emission (Table 2 and Fig. 5).

Free labelled TFOs. As can be seen from Table 2, the λ_{em} for the mono-conjugated TFOs **4** range from 467 nm for $\mathbf{4}_{\mathbf{Th8}}$ to 576 nm for $\mathbf{4}_{\mathbf{42'Q8}}$. Comparison of the fluorescence intensities observed for the mono-conjugated TFOs **4** indicated that they depend on the cyanine composition. For the same concentrations of conjugates, the fluorescence intensity was higher for the thiocyanine derivative, than for the thiazole orange isomers. The quinocyanines gave the lowest signals. The presence of a second label at the 3′-end of the TFOs resulted only in fluorescence intensity changes. For the conjugates $\mathbf{5}_{\mathbf{4TO'8}}$, $\mathbf{5}_{\mathbf{24'Q8}}$ and $\mathbf{6}_{\mathbf{4TO'8.4}}$, fluorescence intensities were not very different from those of the corresponding mono-labelled TFOs. These results can be explained by intra-molecular interactions between the cyanines resulting in significant fluorescence

Table 2 Fluorescence data [a]

TFOs	Free conjugate				Triplex		$F_{Triplex}/F_{TFO}$ [b]	
	λ_{ex}/nm 4 °C	λ_{em}/nm 4 °C	Stokes shift	F_{TFO} 4 °C	λ_{em}/nm 4 °C	$F_{Triplex}$ 4 °C	4 °C	20 °C
$\mathbf{4}_{4TO'8}$	511	527	16	4.81	527	58.32	12.12 (12.13)	24.47 (24.60)
$\mathbf{4}_{4TO'7}$	511	528	17	4.71	528	62.78	13.33 (13.33)	27.63 (27.62)
$\mathbf{4}_{4TO'6}$	513	527	14	7.70	528	56.92	7.39 (7.43)	14.96 (14.97)
$\mathbf{4}_{4TO'5}$	512	528	16	4.14	527	40.12	9.69 (9.71)	15.36 (15.40)
$\mathbf{4}_{4TO'4}$	511	526	15	3.09	525	53.12	17.19 (17.20)	32.20 (32.90)
$\mathbf{4}_{2TO8}$	491	544	53	1.42	531	17.88	12.59 (13.13)	18.29 (18.60)
$\mathbf{4}_{Th8}$	429	467	38	26.26	453	89.26	3.40 (3.70)	5.31 (5.90)
$\mathbf{4}_{2TO'8}$	490	549	59	0.90	550	10.07	11.19 (11.31)	15.57 (15.84)
$\mathbf{4}_{4TO8}$	510	526	16	3.44	527	24.09	7.00 (7.06)	12.73 (12.98)
$\mathbf{4}_{22'Q8}$	527	574	47	0.22	540	5.14	23.36 (27.12)	24.07 (29.84)
$\mathbf{4}_{24'Q8}$	561	572	11	0.70	570	22.75	32.50 (32.83)	37.84 (39.51)
$\mathbf{4}_{42'Q8}$	560	573	13	0.33	576	5.69	17.24 (17.61)	16.11 (19.52)
$\mathbf{5}_{4TO'8}$	512	528	16	5.86	529	54.77	9.35 (9.39)	18.32 (18.54)
$\mathbf{5}_{2TO8}$	459	579	120	4.24	529	28.93	6.82 (12.92)	7.70 (10.02)
$\mathbf{5}_{24'Q8}$	519	583	64	0.58	570	7.77	13.40 (19.15)	7.97 (15.96)
$\mathbf{6}_{4TO'8.4}$	513	528	16	3.00	528	16.26	5.42 (5.45)	6.63 (6.84)

[a] Emission spectra were recorded in a 10 mM sodium phosphate, pH 6, buffer containing 140 mM KCl and 5 mM $MgCl_2$. Concentrations were 1 μM in TFOs and the duplex target. [b] The values indicated are calculated from the intensities measured at the λ_{em} of the triplexes and the λ_{em} of the free labelled TFOs. The values in the brackets correspond to the ratio of intensities measured at the λ_{em} of the triplexes.

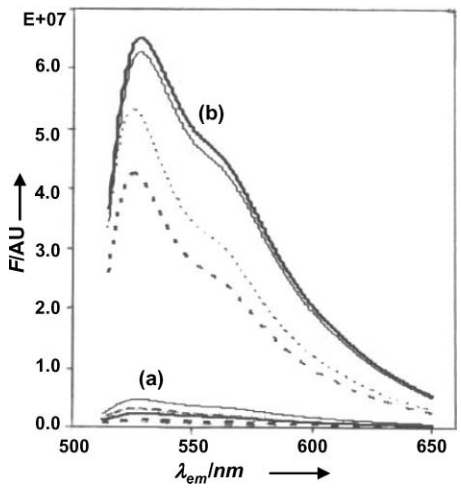

Fig. 5 Fluorescence emission spectra of the free (a) and hybridized (b) 5′-labelled TFOs $\mathbf{4}_{4TO'8}$ (full line) and $\mathbf{4}_{4TO'4}$ (dotted line) in a 10 mM sodium phosphate buffer, pH 6, containing 140 mM KCl, and 5 mM $MgCl_2$ recorded at 20 °C (bold line) and 4 °C (plain line). (Same concentrations and buffer conditions as for Fig 3. λ_{exc} = 465 nm.) Hybridizations were performed overnight.

quenching rates. Comparison of the fluorescence of the conjugates $\mathbf{5}_{4TO'8}$ and $\mathbf{6}_{4TO'8.4}$ indicates that the presence of the longer linker at the 3′-end results in greater quenching. It is possible that in this case the interactions between both **4TO′** units are favoured. These results are in accordance with literature results concerning the bis-labelling of hairpin oligonucleotides with Cy 5.5.[34] For conjugate $\mathbf{5}_{2TO8}$, the presence of a second label resulted in an important red shift of the λ_{em} (from 544 to 579 nm) and an increase in the fluorescence intensity. A comparison of fluorescence intensities for mono-conjugated TFOs **4** and bis-conjugated TFOs **5** and **6** at 4 and 20 °C indicated greater values at the lower temperature (data not shown).

Triplex structures. Upon formation of the triplex structures by hybridization of the conjugates derived from TFOs **4**, **5** and **6** with the double-stranded target, there were either no changes or a very slight shift of the λ_{em} [except for the conjugate $\mathbf{5}_{2TO8}$ (50 nm)] together with a great increase in the fluorescent signal (Table 2). Measurements were performed at 4 and 20 °C. The intensity increases depended on both the cyanine and linker size.

Mono-labelled TFOs. The most important intensity increases upon triplex formation were observed at 20 °C. Among the changes, a 37-fold increase was observed for $\mathbf{4}_{42'Q8}$, 32-fold for $\mathbf{4}_{4TO'4}$, 27-fold for $\mathbf{4}_{4TO'7}$, and 24-fold for $\mathbf{4}_{4TO'8}$. Emission spectra of the free and hybridized TFOs $\mathbf{4}_{4TO'4}$ and $\mathbf{4}_{4TO'7}$ are shown in Fig. 5. Under the same experimental conditions, the hybridization of conjugate $\mathbf{4}_{4TO'8}$ with its complementary single-stranded target $^{5'}$GGGAAAAGAAAATTT$^{3'}$ resulted in only a 30% fluorescence increase, clearly showing the great potential of our new probes for the detection of double-stranded nucleic acid structures (data not shown). It is important to note that when **4TO′** was used as a label, the most important fluorescence increase did not correspond to the more stable triplex structure. In the case of the strongest stabilization, it is likely that its intercalation allowed efficient quenching of the label by the neighboring nucleobases. Conversely, when attached by a shorter linker corresponding to four methylene groups, it is possible that the label could not be fully intercalated. In this case, although the structure formed could block the methine bond rotation, it is possible that it prevented efficient quenching by the nucleobases at the duplex–triplex junction. These results agree with our previous studies obtained with **4TO′**-conjugated oligonucleotides able to detect terminal mismatches on DNA duplexes, with the mismatched duplexes being more fluorescent than the perfect ones.[26]

Bis-labelled TFOs. For modified TFOs involving two cyanines $\mathbf{5}_{4TO'8}$, $\mathbf{5}_{2TO8}$, $\mathbf{5}_{24'Q8}$, and $\mathbf{6}_{4TO'8.4}$, an increase in the fluorescence intensity signal was also observed upon hybridization with the

double-stranded target (18, 10, 15 and 6-fold, respectively). These values are lower than those observed with the corresponding mono-labelled TFOs.

Increasing the fluorescence intensity changes between the free labelled TFO and the triplex structure. In order to increase the difference in the fluorescence emission intensity between the triplex structure and the free labelled TFOs, the possibility of using the strand transfer strategy (Fig. 6) previously reported with single-stranded targets was studied.[35] This method is based on the hybridization of the labelled oligonucleotidic probe with a shorter sequence complementary to the 5′-end, bearing a quencher at its 3′-end. In the presence of the target sequence, strand displacement occurs allowing the hybridization with the latter. In our study, three labelled TFOs $\mathbf{4}_{\mathbf{4TO'8}}$, $\mathbf{4}_{\mathbf{4TO'4}}$ and $\mathbf{5}_{\mathbf{4TO'8}}$ were used. As quenching sequences we used the 10-mer with the complementary sequence to the TFO, $\mathbf{12}_{\mathbf{dab}}$ [5′GAAAAGAAAA*p*-$(CH_2)_6$NH-dabcyl3′] as well as shorter sequences $\mathbf{13}_{\mathbf{dab}}$ [5′AAAGAAAA*p*-$(CH_2)_6$NH-dabcyl3′], $\mathbf{14}_{\mathbf{dab}}$ [5′AAGAAAA*p*-$(CH_2)_6$NH-dabcyl3′] and $\mathbf{15}_{\mathbf{dab}}$ [5′AGAAAA*p*-$(CH_2)_6$NH-dabcyl3′] complementary to the 5′- end of the TFO, bearing a dabcyl residue at their 3′-ends (See Table 1 for characterizations). The quencher was attached by the reaction of its succinimidyl ester with an aminohexyl linker incorporated at the 3′-ends of the oligonucleotides. Each of the labelled TFOs was first hybridized with the series of oligonucleotide–dabcyl conjugates. Fluorescence measurements indicated quenching (up to at least 50%). Then, one equivalent of the double-stranded target was added. Hybridizations were performed in the conditions previously used for triplex formation.

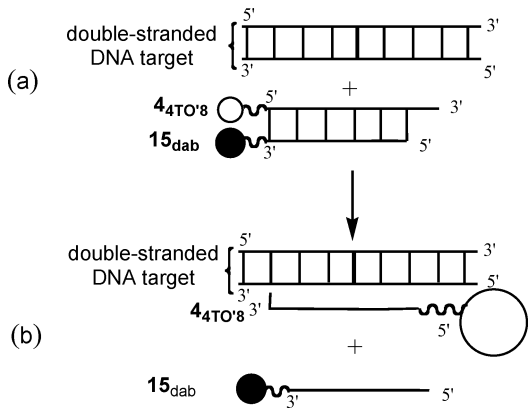

Fig. 6 Schematic representation of the strand transfer from the duplex ($\mathbf{4}_{\mathbf{4TO'8}}$ + $\mathbf{15}_{\mathbf{dab}}$) (a) to the triplex structure (b). The concentrations were 1 μM in each duplex and the buffer was the same as described in Fig. 3.

A large increase in the fluorescence emission was observed when the target was added to the quenched duplex involving the 6-mer-dabcyl conjugate $\mathbf{15}_{\mathbf{dab}}$. The fluorescence intensity of the mixture reached 80% of that observed for the corresponding triplex formed in the absence of $\mathbf{15}_{\mathbf{dab}}$ after 4 h of incubation, indicating the efficiency of the strand transfer. The experiments were performed at 4 and 20 °C. When performed at 20 °C, the strand transfer strategy resulted in a 47-fold fluorescence increase with $\mathbf{4}_{\mathbf{4TO'8}}$ (Fig. 7). In such a strategy, the use of the **4TO′** labelled TFO involving the eight methylene linker forming the more stable triplex structure was required for efficient strand transfer. This result is in accordance with the T_m values observed for the duplexes

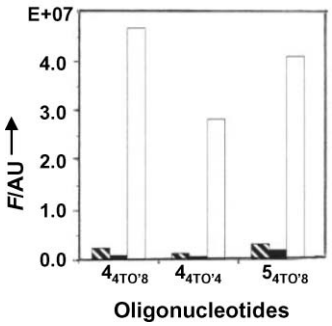

Fig. 7 Fluorescence intensities for the free conjugates (hatched), the quenched duplex (labelled TFO + $\mathbf{15}_{\mathbf{dab}}$) (black) and the quenched duplex in the presence of the DNA target (**1** + **2**) (white). Concentrations and buffer conditions were the same as for Fig. 3. Experiments were performed at 20 °C.

$\mathbf{4}_{\mathbf{4TO'8}}$ + $\mathbf{15}_{\mathbf{dab}}$ and $\mathbf{4}_{\mathbf{4TO'4}}$ + $\mathbf{15}_{\mathbf{dab}}$ (23.5 °C and 18 °C, respectively), and those of the corresponding triplexes (37.5 °C and 26.6 °C, respectively).

Other sequence contexts

In order to test the ability of our labelling method to detect triplex structures in different contexts, we have designed and synthesized other TFOs labelled at their 5′-end with TO′ *via* an eight methylene linker (Table 3). We chose, first, a 17-mer pyrimidine TFO involving a cytosine at the 5′-end **16**. The synthesis was performed as reported for the synthesis of the conjugates of **4** (see Table 1 for characterizations). This TFO was designed to hybridize with 17-contiguous purines on a double-stranded DNA of 26 base-pairs (triplex **I**). Other double-stranded targets were also chosen in order to allow mismatched triplex formation. Mutations were incorporated on either the purine or the pyrimidine strands at different positions to give either terminal or internal mismatched triplexes (triplexes **II** to **V**). Another 5′-TO′ labelled 17-mer pyrimidine TFO **17** was designed to bind to a duplex target involving an AT base-pair inversion at an internal position (triplex **VI**). On the basis of literature indicating that the mismatched GTA triplet was among the least destabilizing,[36–38] we chose to incorporate a guanine in the TFO in the position facing the AT base-pair inversion. The stability provided by the TO′ labelling in these different contexts was evaluated by thermal denaturation studies followed by absorption spectroscopy using the corresponding unlabelled triplexes as references. Fluorescence intensity changes observed upon hydridization were determined by steady-state experiments.

Absorption studies. The longer length of the duplex target allowed us to distinguish between the triplex-to-duplex and the duplex-to-single strand transitions. The T_m value for the fully matched triplex **I** is 41.5 °C (T_m value for the fully matched duplex is 69.5 °C). The presence of mismatches in the triplex structures induced different effects that depended on both their position on the triplexes (terminal *versus* internal position) and the strand where mutations were incorporated (pyrimidine *versus* purine strand). In agreement with the literature,[36–38] our results indicated that the incorporation of a purine base in the pyrimidine strand, which affects only the Watson and Crick (WC) base-pair

Table 3 T_m and fluorescence data for the 17-mer triplexes **I–VI**

17-mer Triplexes [a]	T_m/°C [b] (±0.5 °C)	ΔT_m/°C [c] (±1 °C)	F_{TFO} [d] 4 °C	F_{TFO} [d] 25 °C	$F_{Triplex}$ 4 °C	$F_{Triplex}$ 25 °C	$F_{Triplex}/F_{TFO}$ [e] 4 °C	$F_{Triplex}/F_{TFO}$ [e] 25 °C
Fully matched triplex I								
$^{3'}$CCCGACTTCTTTTTCTTTCTTCGCGC$^{5'}$	69.5	—	—	—	—	—	—	—
$^{5'}$GGGCTGAAGAAAAAGAAAGAAGCGCG$^{3'}$								
$^{5'}$CTTCTTTTTCTTTCTTC$^{3'}$ **16**	41.5	—	—	—	—	—	—	—
4TO′-$(CH_2)_8$-S-*p* $^{5'}$CTTCTTTTTCTTTCTTC$^{3'}$ **16$_{4TO'8}$**	47.5	—	6.76	1.48	28.56	20.41	4.22	13.79
(WC) Mismatched triplex (end) II								
$^{3'}$CCCGA**A**TTCTTTTTCTTTCTTCGCGC$^{5'}$	65	*–4.5*	—	—	—	—	—	—
$^{5'}$GGGCT**G**AAGAAAAAGAAAGAAGCGCG$^{3'}$								
$^{5'}$**C**TTCTTTTTCTTTCTTC$^{3'}$ **16**	41.5	*0*	—	—	—	—	—	—
4TO′-$(CH_2)_8$-S-*p* $^{5'}$**C**TTCTTTTTCTTTCTTC$^{3'}$ **16$_{4TO'8}$**	46.5	*–1*	6.76	1.48	20.82	14.65	3.08	9.90
(WC) Mismatched triplex (internal) III								
$^{3'}$CCCGACTTCTTT**G**TCTTTCTTCGCGC$^{5'}$	66	*–3.5*	—	—	—	—	—	—
$^{5'}$GGGCTGAAGAAA**A**AGAAAGAAGCGCG$^{3'}$								
$^{5'}$CTTCTTTT**T**CTTTCTTC$^{3'}$ **16**	40	*–1.5*	—	—	—	—	—	—
4TO′-$(CH_2)_8$-S-*p* $^{5'}$CTTCTTTT**T**CTTTCTTC$^{3'}$ **16$_{4TO'8}$**	44	*–3.5*	6.76	1.48	28.50	20.19	4.21	13.64
(WC + H) Mismatched triplex (end) IV								
$^{3'}$CCCGA**C**TTCTTTTTCTTTCTTCGCGC$^{5'}$	63.5	*–6*	—	—	—	—	—	—
$^{5'}$GGGCT**T**AAGAAAAAGAAAGAAGCGCG$^{3'}$								
$^{5'}$**C**TTCTTTTTCTTTCTTC$^{3'}$ **16**	39	*–2.5*	—	—	—	—	—	—
4TO′-$(CH_2)_8$-S-*p* $^{5'}$**C**TTCTTTTTCTTTCTTC$^{3'}$ **16$_{4TO'8}$**	45.5	*–2*	6.76	1.48	19.42	13.66	2.87	8.55
(WC + H) Mismatched triplex (internal) V								
$^{3'}$CCCGACTTCTTT**T**TCTTTCTTCGCGC$^{5'}$	62	*–7.5*	—	—	—	—	—	—
$^{5'}$GGGCTGAAGAAA**C**AGAAAGAAGCGCG$^{3'}$								
$^{5'}$CTTCTTTT**T**CTTTCTTC$^{3'}$ **16**	nd		—	—	—	—	—	—
4TO′-$(CH_2)_8$-S-*p* $^{5'}$CTTCTTTT**T**CTTTCTTC$^{3'}$ **16$_{4TO'8}$**	26[f]		6.76	1.48	23.71	6.81	3.51	4.60
bp inversion on duplex (internal) VI								
$^{3'}$CCCGACTTCTTT**A**TCTTTCTTCGCGC$^{5'}$	68.5	*–1*	—	—	—	—	—	—
$^{5'}$GGGCTGAAGAAA**T**AGAAAGAAGCGCG$^{3'}$								
$^{5'}$CTTCTTT**G**TCTTTCTTC$^{3'}$ **17**	33	*–8.5*	—	—	—	—	—	—
4TO′-$(CH_2)_8$-S-*p* $^{5'}$CTTCTTT**G**TCTTTCTTC$^{3'}$ **17$_{4TO'8}$**	38.5	*–9*	12.32	3.16	29.08	20.40	2.36	6.46

[a] Mismatched triplets are indicated in bold characters. [b] T_m values for the duplexes, the unlabelled and labelled triplexes formed by the labelled TFOs in a 10 mM sodium phosphate, pH 6, buffer containing 140 mM KCl and 5 mM $MgCl_2$. Concentrations were 1 μM in the duplex target and TFOs. [c] ΔT_m were calculated using the perfect duplexes, unlabelled triplexes and labelled triplexes as references. [d] Fluorescence intensities for the free labelled TFOs and the corresponding triplexes. [e] Ratio intensities measured at the λ_{em} of the triplexes. [f] A transition with a weak intensity was observed.

formation, had either no (triplex **II**) or only a moderate effect on the triplex stabilities (triplex **III**) while the incorporation of a pyrimidine base in the purine strand had a greater destabilizing effect (triplexes **IV** and **V**). In addition to its effect on the Watson and Crick (WC) base-pair formation, this kind of modification also altered the Hoogsteen base-pairing. In this case, the stability of the triplex involving a mismatch at the end (triplex **IV**) is decreased by 2.5 °C while no triplex was detected, under the experimental conditions used, when a pyrimidine was incorporated at an internal position. The hybridization of the 17-mer TFO **17**, containing a guanine, with the duplex involving an AT base-pair inversion also resulted in the formation of a triplex (triplex **VI**) but with decreased stability (by 8.5 °C) as compared with that of the perfectly matched one (triplex **I**). In all cases, labelling the TFOs with the intercalator thiazole orange TO′ induced the formation of triplexes with increased stabilities as compared with the unlabelled ones. However, the stability increase due to labelling of the TFOs was reduced when the size of the triplex was increased from 10 to 17 base-triplets. Similar trends were also previously observed with other intercalators such as acridine and perylene.[10,19,25] A comparison of the stabilities of the labelled triplexes with those of the corresponding unlabelled ones clearly showed that the binding specificity was not reduced due to the presence of the stabilizing label. A stability increase of +6 °C was observed for the fully matched triplex (**I**) and +5.5 °C for the triplex involving the AT base-pair inversion (**VI**). Similar stability increases were also observed for triplexes **II** and **III** involving the terminal mismatches and the triplex with the internal mutation on the pyrimidic strand (triplex **IV**). When the mutation was incorporated in the purine strand (triplex **V**) the presence of the label induced the formation of a triplex structure but with low stability ($T_m = 26$ °C) as compared with those of the other triplexes.

Fluorescence studies. A comparison of the fluorescence intensities emitted by the free labelled TFOs indicated that they depend on both their length and base composition. The fluorescence of the 17-mer pyrimidine TFO **16$_{4TO'8}$** was 1.4-fold higher than that of the 10-mer TFO **4TO′8**. The replacement of a thymine by a

guanine in the TFO $\mathbf{17}_{\mathbf{4TO'8}}$ led to a further increase (about 2-fold) in the fluorescence emission. This can be explained by the back-binding effect previously reported for thiazole orange labelled peptide nucleic acids and oligonucleotides.[39,14] The fluorescence emissions of the purine rich oligonucleotides labelled with thiazole orange were also higher than those in the pyrimidine series due to stronger stacking interactions between the purine rings and the thiazole orange.[39–41] Furthermore, in the case of TFO $\mathbf{17}_{\mathbf{4TO'8}}$, the concomitant presence of the intercalating molecule and the possibility of an internal GC base-pair formation was an additional factor in favor of the back-binding structure. Upon an increase in temperature, a decrease in the fluorescence emission was observed (Table 3 and data not shown). Upon hybridization of the labelled TFOs with the different duplexes, fluorescence emission increases were observed in all cases. A comparison of the results obtained at 4 °C and 25 °C indicated that the intensities were greater at a lower temperature (4 °C *versus* 25 °C). However, the following observations can be made. At 4 °C, the fluorescence intensities of triplexes **I**, **III** and **VI** were nearly identical while that of triplex **V** with weak stability, was weaker. The weakest fluorescence intensities were observed for the triplexes **II** and **IV** involving mismatched triplets in the position adjacent to the intercalation site at the duplex to triplex junction. When the experiments were performed at 25 °C, the fluorescence intensities were decreased by a third for all the triplexes except for triplex **V** for which a more important reduction was observed (more than two thirds). The resulting fluorescence intensity ratio at 25 °C, between the triplex structures and the labelled TFOs, was ~13.7 fold for fully matched triplex **I** and triplex **III** involving a mutation at an internal position on the pyrimidine strand. Due to the presence of the terminal mismatches, the ratio was slightly weaker for triplexes **II** and **IV** (9.9-fold and 8.5-fold, respectively, Fig. 8) while it was the weakest for triplex **V** with the mutation at an internal position of the purine strand. For triplex **VI** with the AT base-pair inversion, the ratio was only 6.5-fold due to the high fluorescence intensity of the free labelled TFO $\mathbf{17}_{\mathbf{4TO'8}}$. These results confirm the possibility of detection of double-stranded nucleic acid structures by triple-helix formation with thiazole orange 5′-labelled TFOs.

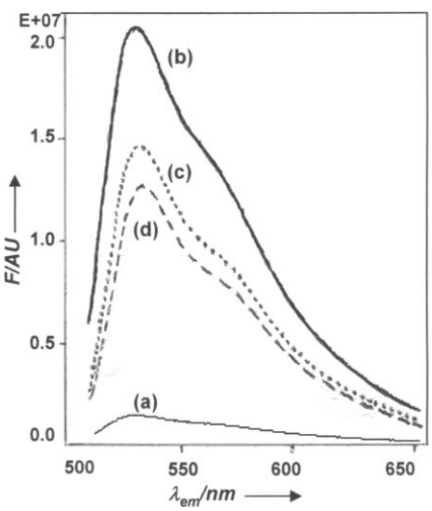

Fig. 8 Fluorescence emission spectra of the free 5′-labelled TFO **16** (a), fully matched triplex **I** (b) and end-mismatched triplexes **II** (c) and **IV** (d) in a 10 mM sodium phosphate buffer, pH 6, containing 140 mM KCl, and 5 mM $MgCl_2$ recorded at 25 °C (same concentrations and buffer conditions as for Fig 3. $\lambda_{exc} = 465$ nm.) Hybridizations were performed overnight.

Conclusion

We have reported the possibility of detecting double-stranded nucleic acid sequences by hybridization of "light-up" TFOs involving fluorescent labels with intercalating properties. These labels are monomethine cyanines. One thiocyanine, four thiazole orange isomers and three quinocyanines were linked to the 5′-end of a 10-mer pyrimidine TFO. The binding properties of these labelled TFOs with the double-stranded nucleic acid target, studied by absorption and steady-state fluorescence spectroscopies, indicated that strong stability can be obtained by choosing a convenient linker size. Stability also depends on the label structure. The presence of one benzothiazole ring is required to obtain good stability. The linkage of a second label at the 3′-end of the TFOs provides additional stability. Steady-state fluorescence experiments showed an important intensity increase upon triplex formation. While the most important fluorescence increase was observed with a quinocyanine (37-fold), the conjugates involving thiazole orange attached by the benzothiazole ring provided the most balanced properties in terms of triplex stabilization, fluorescence intensity and fluorescence enhancement upon hybridization with the double-stranded target. It is also possible to increase the fluorescence emission upon triplex formation by quenching the fluorescence of the labelled TFO by its hybridization with a shorter sequence complementary to the 5′-end of the TFO and bearing a quencher at its 3′-end. Due to the stabilizing properties of the labels, strand displacement occurs resulting in the formation of a triplex structure. Formation of the triplex is accompanied by a strong fluorescence enhancement (up to about 47-fold). The formation of longer fully matched triplex structures (17 triplets) also induced an important fluorescence increase (13-fold), while the presence of a mismatched base-pair on the duplex, at the duplex–triplex junction, resulted in a reduced fluorescence increase. A 17-mer TO′-labelled TFO involving a guanine facing an AT inversion on the duplex target also formed a triplex structure detectable by a large fluorescence enhancement (6.5-fold). These new "light up" TFOs (LU-TFOs) will be useful tools for the detection of specific sequences on double-stranded nucleic acids.

Experimental

General methods

All solvents used were of the highest purity and did not contain more than 10 ppm H_2O. All chemicals were used as obtained unless otherwise stated. During all the syntheses and purification steps cyanine-linker derivatives and TFO–cyanine conjugates were protected from light. Analytical thin-layer chromatography (TLC) was performed on precoated alumina plates (Merck silica gel 60F 254 ref. 5554). For flash chromatography, Merck silica gel 60 (40–63 μM) (ref. 9385 from Merck) was used. NMR spectroscopy was performed on a Varian Unity 500 spectrometer. ^{1}H chemical shifts were referenced to Me_4Si. ^{1}H NMR coupling constants are reported in Hz and refer to apparent multiplicities. Mass analysis was performed on a Quattro II (Micromass) instrument. TFOs were synthesized using cyanoethyl phosphoramidite chemistry

and an Expedite nucleic acid synthesis system 8909 from Perseptive Biosystems. Reversed-phase chromatography and purification were performed on a 600 E (System Controller) equipped with a photodiode array detector (Waters 990) using a LiChrospher 100 RP 18 (5 μm) column (125 mm × 4 mm) from Merck. Analyses and purifications by ion-exchange chromatography were carried out on a Pharmacia FPLC with a MonoQ (8 μm, 10 × 100 mm, Pharmacia). UV spectra were recorded on an Uvikon 860 spectrophotometer. Fluorescence spectra were recorded on a Fluoromax 2 (ISA-Jobin-Yvon) spectrofluorimeter in 0.5 cm path-length Suprasil quartz cuvettes (Hellma) with slits set at 0.5 mm (band pass = 2 nm). Oligonucleotides **1**, **2**, **3** and the 26-mer oligonucleotides were from Eurogentec. Their concentrations were calculated using molar extinction coefficients at 260 nm, determined by the nearest-neighbor model.[42]

Synthesis

Synthesis of the cyanine-linker derivatives. The syntheses of cyanine-linker derivatives **4TO′**-$(CH_2)_n$-I (n = 4, 5, 6, 7 and 8), **2TO**-$(CH_2)_8$-I, **2Th**-$(CH_2)_8$-I, **2TO′**-$(CH_2)_8$-I, **4TO**-$(CH_2)_8$-I, **22′Q**-$(CH_2)_8$-I, **24′Q**-$(CH_2)_8$-I, and **42′Q**-$(CH_2)_8$-I were performed as previously described.[14,26]

Synthesis of the 5′-thiophosphorylated TFO 4 (Scheme 1a). The TFO was assembled at the 1 μmol scale. At the end of the chain assembly an additional detritylation step was performed followed by the incorporation of the thiophosphate group according to our previously reported procedure.[30] TFO **4** was purified by reversed-phase chromatography using a linear gradient of CH_3CN (5 to 50% over 60 min) in 0.1 M aqueous ammonium acetate, pH 7, with a flow rate of 1 cm^3 min^{-1}.

Synthesis of the bis 3′-,5′-bis-thiophosphorylated TFO 5 (Scheme 1b). The synthesis was performed at the 1 μmol scale on our previously reported modified support **8** leaving, after the deprotection step, a thiophosphate group at the 3′-end.[31] At the end of the chain assembly an additional detritylation step and the incorporation of the thiophosphate group were performed following our previously reported procedure.[30] TFO **5** was purified by ion-exchange chromatography using a linear gradient of NaCl in a 25 mM Tris–HCl buffer, pH 7, containing 10% MeOH. Yield (30%).

Synthesis of the 3′-thiolated-,5′-thiophosphorylated TFO 6 (Scheme 2). The synthesis was performed at the 1 μmol scale on modified support **11** described below. At the end of the chain assembly an additional detritylation step and the incorporation of the thiophosphate group at the 5′-end were performed as described above. TFO **6** was purified by ion-exchange chromatography using the conditions reported above. Yield (31%).

The synthesis of the modified support involving a masked thiol function **11** was obtained as follows. A solution of thiohexanol **9** (5 g, 37.25 mmol) in EtOH–NH_4OH (1 : 2, v/v), (30 cm^3) was stirred with air bubbling for ten days with addition of NH_4OH (2 cm^3) every two days to give the 6,6′-dithiodihexanol. The mixture was concentrated to dryness and then purified on a silica gel column using a MeOH gradient (0 to 3%) in CH_2Cl_2 to give a white powder (1.7 g, 6.4 mmol, 35%). R_f = 0.30 (CH_2Cl_2–MeOH, 90 : 10, v/v). ESI-MS: m/z, $C_{12}H_{26}O_2S_2$, calc. 266.46, found 265.40 (M^-).

A solution of 4,4′-*O*-dimethoxytritylchloride (550 mg, 1.65 mmol, 0.27 eq.) in pyridine (20 cm^3) was then added to 6,6′-dithiodihexanol (1.65 g, 1 eq., 6.2 mmol) previously dried by coevaporation with anhydrous pyridine. After 5 h of stirring at rt, 4,4′-*O*-dimethoxytritylchloride (0.1 eq., 51 mg, 0.15 mmol) was added and the stirring was continued overnight. The pyridine was azeotroped with toluene and the residue purified on a silica gel column using a MeOH gradient (0 to 3%) in CH_2Cl_2 to give **10** as yellow oil (950 mg, 1.6 mmol, 95%). R_{f14} = 0.55 (CH_2Cl_2–MeOH, 90 : 10, v/v). ^{1}H NMR (500 MHz, $CDCl_3$, TMS) δ = 7.45 (2H, d, $^4J_{H\text{-}H}$ = 7.3 Hz, -ODMT), 7.33 (4H, d, $^4J_{H\text{-}H}$ = 8.9 Hz, -ODMT), 7.29 (2H, m, -ODMT), 7.21 (1H, t, $^3J_{H\text{-}H}$ = 7.1 Hz, -ODMT), 6.83 (4H, d, $^4J_{H\text{-}H}$ = 8.9 Hz, -ODMT), 3.80 (6H, s, -ODMT), 3.64 (2H, t, $^3J_{H\text{-}H}$ = 6.5 Hz, -CH_2ODMT), 3.05 (2H, t, $^3J_{H\text{-}H}$. = 6.5 Hz, -CH_2OH), 2.68 (4H, dd, $^3J_{H\text{-}H}$ = 7.5 Hz, $^3J_{H\text{-}H}$ = 9 Hz, -CH_2-SS-CH_2-), 1.68 (4H, m, -CH_2CH_2S-SCH_2CH_2-), 1.60 (4H, m, -CH_2CH_2OH + -CH_2CH_2ODMT), 1.40 [8H, m, -$(CH_2)_n$-]. ESI-MS: m/z, $C_{33}H_{44}O_4S_2$, calc. 568.84, found 591.73 ($M + Na^+$). 1-*O*-Dimethoxytrityl-6,6′-dithiodihexanol **10** (900 mg, 1.6 mmol, 1 eq.), succinic anhydride (159 mg, 1.59 mmol, 0.95 eq.) and 4-dimethylaminopyridine (183 mg, 1.5 mmol, 0.9 eq.) were solubilized with anhydrous pyridine (12 cm^3) and the mixture was stirred for 24 h at rt. The pyridine was azeotroped with toluene. The residue was washed with a 10% aqueous citric acid solution (10 cm^3) and H_2O (10 cm^3) then extracted with CH_2Cl_2 (3 × 20 cm^3). The organic phase was dried over magnesium sulfate and concentrated. Brown oil. (1.04 g, 1.52 mmol) Yield: 95%. R_f = 0.35 (CH_2Cl_2–MeOH, 90 : 10, v/v). ESI-MS: m/z, $C_{37}H_{48}O_7S_2$, calc. 668.90, found 667.49 (M^-). Functionalization of the support was then performed as previously reported[31] by replacing the 1-*O*-dimethoxytrityloxyethyl-1′-succinyl-ethyl-2,2′-disulfide with 1-*O*-dimethoxytrityl-6,6′-dithiodihexanol **10** and aminopropyl fractosil with LCCA-CPG 500 Å (Chemgenes). Loading 36 μmol g^{-1}.

Labelling of 5′- and bis 3′-,5′-thiophosphorylated TFOs 4, 5, 16 and 17. DMF solutions of the selected cyanine-linker derivatives (1.5 mg in 0.3 cm^3, 10 eq.) were added to vortexed solutions of 5′-thiophosphorylated TFOs **4**, **5**, **16** and **17** (10 OD each) in a 2.5% aqueous bicarbonate buffer, pH = 9, (0.2 cm^3). The mixture was stirred for 4 to 10 h at rt. The coupling efficiency was monitored by reversed-phase analysis using the same conditions as described above. TFO–cyanine conjugates were obtained with increased retention times as compared to those of the starting TFOs **4** or **5**. During the entire work-up, conjugate solutions were protected from light. Mixtures were evaporated to dryness under reduced pressure. The residue was dissolved with water (2 cm^3) and extracted several times with CH_2Cl_2. The aqueous phase was passed over a size exclusion Sephadex G 10 column, using water as the eluant. Fast eluting colored fractions were purified by reversed-phase chromatography with a linear gradient of CH_3CN (5% to 50% over 60 min for mono-labelled conjugates and bis-labelled conjugates) in 0.1 M aqueous ammonium acetate, pH 7, with a flow rate of 1 cm^3 min^{-1}. (See Table 1 for retention times and mass analysis data.) Yields were: $\mathbf{4}_{\mathbf{Th8}}$ (37%), $\mathbf{4}_{\mathbf{2TO'8}}$ (32%), $\mathbf{4}_{\mathbf{4TO'8}}$ (30%), $\mathbf{4}_{\mathbf{2TO8}}$ (27%), $\mathbf{4}_{\mathbf{4TO8}}$ (35%), $\mathbf{4}_{\mathbf{22'Q8}}$ (48%), $\mathbf{4}_{\mathbf{24'Q8}}$ (28%), $\mathbf{4}_{\mathbf{42'Q8}}$ (40%), $\mathbf{5}_{\mathbf{4TO'8}}$ (27%), $\mathbf{5}_{\mathbf{2TO8}}$ (40%), $\mathbf{5}_{\mathbf{24'Q8}}$ (25%), $\mathbf{16}_{\mathbf{4TO'8}}$ (25%) and $\mathbf{17}_{\mathbf{4TO'8}}$ (20%). Electrospray mass analysis confirmed the mass of all the conjugates.

Bis-labelling of the 3′-thiolated,5′-thiophosphorylated TFO 6. 5′-Labelling was performed as described for the labelling of TFOs **4**, and **5** using 20 OD of TFO **6** and the **4TO′**-$(CH_2)_8$-I cyanine-linker derivative. After purification of the 5′-labelled TFO by reversed-phase chromatography, the organic solvent was removed by evaporation and the buffer by lyophilization. The solution of 5′-labelled TFO **6** in a 2.5% aqueous bicarbonate buffer, pH = 9, (0.2 cm^3) was degassed for 15 min by a stream of argon. Then, a degassed TCEP[32] solution (5 mg in 0.75 cm^3) in a 2.5% aqueous bicarbonate buffer, pH = 9, (0.02 cm^3) was added. After 10 min, a degassed DMF solution of **4TO′**-$(CH_2)_4$-I (1.5 mg in 0.3 cm^3) was added and the mixture vigorously vortexed. After 2 h of reaction, the coupling efficiency was monitored by reversed-phase analysis using the same conditions as described above. During the entire work-up, the conjugate solutions were protected from light. Mixtures were evaporated to dryness using a toluene–DMF azeotrope. The residue was dissolved with a 1 M NaCl solution in H_2O–MeOH (80 : 20, v/v) (2 mL) and extracted several times with CH_2Cl_2. The aqueous phase was passed over a size exclusion Sephadex G10 column, using water as the eluant. Fast eluting colored fractions were purified by reversed-phase chromatography using the conditions described above. (See Table 1 for retention times and mass analysis data.) The bis-conjugated $\mathbf{6}_{\mathbf{4TO'8.4}}$ was purified by reversed-phase chromatography using the conditions described *vide supra.* Yield (5%).

Synthesis of the ON–dabcyl conjugates. ONs involving an aminohexyl linker at the 5′-end were synthesized at the 1 μmol scale on a previously reported modified support.[43] Deprotection and purification was then performed by ion-exchange chromatography as reported above. A DMF solution of dabcyl succinimidyl ester (1.5 mg in 0.3 cm^3, 10 eq.) was added to vortexed solutions of 3′-aminohexyl-ONs (10 OD each) in a 2.5% aqueous bicarbonate buffer, pH = 9 (0.2 cm^3). The mixture was stirred for 4 h at rt. The coupling efficiency was monitored by reversed-phase analysis using the same conditions as described above. ON–dabcyl conjugates $\mathbf{12}_{\mathbf{dab}}$, $\mathbf{13}_{\mathbf{dab}}$, $\mathbf{14}_{\mathbf{dab}}$ and $\mathbf{15}_{\mathbf{dab}}$ were obtained with increased retention times as compared with the starting 3′-aminohexyl-oligonucleotide conjugates. During the entire work-up, conjugate solutions were protected from light. Mixtures were evaporated to dryness under reduced pressure. The residue was dissolved with water (2 cm^3) and extracted several times with CH_2Cl_2. The aqueous phase was passed over a size exclusion Sephadex G 10 column using water as the eluant. Fast eluting colored fractions were purified by reversed-phase chromatography with a linear gradient of CH_3CN (5% to 50% over 60 min) in 0.1 M aqueous ammonium acetate, pH 7, with a flow rate of 1 cm^3 min^{-1}. (See Table 1 for retention times and mass analysis data.) Yields were $\mathbf{12}_{\mathbf{dab}}$ (60%), $\mathbf{13}_{\mathbf{dab}}$ (55%), $\mathbf{14}_{\mathbf{dab}}$ (70%) and $\mathbf{15}_{\mathbf{dab}}$ (75%). Electrospray mass analysis confirmed the mass of all conjugates.

Absorption studies

Molar absorption coefficient determination. The molar absorption coefficients (ε_{260nm} values) for the conjugates derived from TFOs **4**, **16** and **17** were estimated to be the sum of the ε values of the TFO and cyanines deducted from ref. 14 (see Table 1). The same ε_{260nm} values were used for the series of conjugates $\mathbf{4}_{\mathbf{4TO}n}$ involving different linker sizes (n = 4, 5, 6, 7 and 8). The molar extinction coefficients (ε) for conjugates of **5** were determined by titrating the conjugate solutions in a 10 mM sodium phosphate, pH 6, buffer containing 100 mM NaCl at 5 °C with a solution of the single-stranded complementary sequence $^{5'}$GGGAAAAGAAAATTT$^{3'}$. The molar extinction coefficients (ε) for oligonucleotide–dabcyl conjugates $\mathbf{12}_{\mathbf{dab}}$, $\mathbf{13}_{\mathbf{dab}}$, $\mathbf{14}_{\mathbf{dab}}$ and $\mathbf{15}_{\mathbf{dab}}$ were determined by titrations with the complementary sequence **3**.

***T_m* measurements.** The T_m values for the triplex formed by the mono- and bis-labelled TFOs and the double-stranded target **1** + **2** were determined by thermal denaturation followed by absorption spectroscopy using 1 μM solutions of TFOs and 1 μM of the double-stranded duplex in a 10 mM KH_2PO_4 buffer (pH 6), containing 140 mM KCl and 5 mM $MgCl_2$. The samples were left to hybridize overnight at 4 °C (far below the T_m value) in the dark. Results are given in Table 1. The uncertainty in the T_m values reported was ±1 °C.

Fluorescence studies

Fluorescence excitation and emission spectra were recorded on a Fluoromax 2 (ISA-Jobin-Yvon) spectrofluorimeter in 0.5 cm path-length Suprasil quartz cuvettes (Hellma) with slits set at 0.5 mm (band pass = 2 nm). A 1 μM solution of labelled TFOs was prepared in a 10 mM KH_2PO_4 buffer (pH 6), containing 140 mM KCl and 5 mM $MgCl_2$ The triple-stranded samples were prepared by the addition of a small volume (0.005 cm^3) of a concentrated solution of the target (1 eq.) at rt. The sample was left to hybridize overnight at 4 °C, 20 °C or 25 °C in the dark before the measurements were performed. The fluorescence emission spectra of free and hybridized labelled TFOs were recorded between λ = 450 and 700 nm. Errors in fluorescence values were estimated to be ±10%.

Acknowledgements

We thank the Region Centre for a doctoral fellowship to Brice-Loïc Renard. We thank the "Plateforme de Spectrometrie de masse" of the "Centre de Biophysique Moléculaire" for analysis facilities, C. Buré and G. Gaband for running the mass spectrometers and H. Meudal for recording the NMR spectra.

References

1 A. Okamoto, Y. Saito and I. Saito, *Photochem. Photobiol., C*, 2005, **6**, 108.
2 R. Ranasinghe and T. Brown, *Chem. Commun.*, 2005, 5487.
3 U. Asseline, *Curr. Org. Chem.*, 2006, **10**, 491.
4 J. N. Wilson and E. T. Kool, *Org. Biomol. Chem.*, 2006, **4**, 4265.
5 K. E. Sapsford, L. Berti and I. L. Medintz, *Angew. Chem., Int. Ed.*, 2006, **45**, 4562.
6 A. A. Marti, S. Jockusch, N. Stevens, J. Ju and N. J. Turro, *Acc. Chem. Res.*, 2007, **40**, 402.
7 J. L. Mergny, T. Garestier, M. Rougée, A. V. Lebedev, M. Chassignol, N. T. Thuong and C. Hélène, *Biochemistry*, 1994, **33**, 15321.
8 T. Inoue, Y. Sugiura, J. Saitoh, T. Ishiguro and M. Otsuka, *Bioorg. Med. Chem.*, 1999, **7**, 1207.
9 G. N. Grimm, A. S. Boutorine, P. Lincoln, B. Norden and C. Hélène, *ChemBioChem*, 2002, **3**, 324.
10 Y. Aubert and U. Asseline, *Org. Biomol. Chem.*, 2004, **2**, 3496.
11 H. Kuhn, *Antisense Nucleic Acid Drug Dev.*, 2001, **11**, 265.
12 J. S. Sun and C. Hélène, *Nucleosides, Nucleotides Nucleic Acids*, 2003, **22**, 489.

13 E. Brunet, M. Corgnali, L. Perrouault, V. Roig, U. Asseline, M. D. Sorensen, B. R. Babu, J. Wengel and C. Giovannangeli, *Nucleic Acids Res.*, 2005, **33**, 4223.
14 R. Lartia and U. Asseline, *Chem.–Eur. J.*, 2006, **12**, 2270.
15 L. G. Lee, C.-H. Chen and L. A. Liu, *Cytometry*, 1986, **7**, 508.
16 J. Nygren, N. Svanvik and M. Kubista, *Biopolymers*, 1998, **46**, 39.
17 S. Prodhomme, J.-P. Demaret, S. Vinogradov, U. Asseline, L. Morin-Allory and P. Vigny, *J. Photochem. Photobiol., B*, 1999, **53**, 60.
18 A. Larsson, C. Carlsson, M. Jonsson and B. Albinsson, *J. Am. Chem. Soc.*, 1994, **117**, 8459.
19 U. Asseline and E. Cheng, *Tetrahedron Lett.*, 2001, **42**, 9005.
20 S. Vinogradov, V. Roig, Z. Sergueeva, C.-H. Nguyen, P. Arimondo, J.-S. Sun, N. T. Thuong, E. Bisagni, C. Hélène and U. Asseline, *Bioconjugate Chem.*, 2003, **76**(14), 120.
21 D. A. Collier, J.-L. Mergny, N. T. Thuong and C. Hélène, *Nucleic Acids Res.*, 1991, **19**, 4219.
22 U. Asseline, N. T. Thuong and C. Helene, *New J. Chem.*, 1997, **21**, 5.
23 J. S. Sun, C. Giovannangeli, J. C. François, R. Kurfürst, T. Montenay-Garestier, U. Asseline, N. T. Thuong and C. Hélène, *Proc. Natl. Acad. Sci. U. S. A.*, 1991, **88**, 6023.
24 U. Asseline, E. Bonfils, D. Dupret and N. T. Thuong, *Bioconjugate Chem.*, 1996, **7**, 369.
25 U. Asseline, M. Delarue, G. Lancelot, F. Toulme, N. T. Thuong, T. Montenay-Garestier and C. Helene, *Proc. Natl. Acad. Sci. U. S. A.*, 1984, **81**, 3297.
26 U. Asseline, M. Chassignol, Y. Aubert and V. Roig, *Org. Biomol. Chem.*, 2006, **4**, 1949.
27 T. Montenay-Garestier, J. S. Sun, J. Chomilier, J. L. Mergny, M. Takasugi, U. Asseline, N. T. Thuong, M. Rougee and C. Helene, in "*Molecular basis of specificity in nucleic acid-drug interactions*" ed. B. Pullman and J. Jortner, Kluwer Academic Publishers, The Netherlands, 1990, p. 275.
28 N. T. Thuong and U. Asseline, in *Current Protocols in Nucleic Acid Chemistry*. ed. S. Beaucage, D. E. Bergstrom, G. D. Glick and R. A. Jones. John Wiley & Sons, New York, 2000, pp. 4.2.1–4.2.34.
29 S. L. Beaucage and M. H. Caruthers, *Tetrahedron Lett.*, 1981, **22**, 1859.
30 R. Lartia and U. Asseline, *Tetrahedron Lett.*, 2004, **45**, 949.
31 U. Asseline, E. Bonfils, R. Kurfürst, M. Chassignol, V. Roig and N. T. Thuong, *Tetrahedron*, 1992, **48**, 1233.
32 J. A. Burns, J. C. Butler, J. Moran and G. M. Whitesides, *J. Org. Chem.*, 1991, **56**, 2648.
33 D. A. Gianolio, J. M. Segismundo and L. McLaughlin, *Nucleic Acids Res.*, 2000, **28**, 2128.
34 V. Metelev, R. Weissleder and A. Bogdanov Jr, *Bioconjugate Chem.*, 2004, **15**, 1481.
35 Q. Li, G. Luan, Q. Guo and J. Liang, *Nucleic Acids Res.*, 2002, **30**, e5.
36 J.-S. Sun, J.-L. Mergny, R. Lavery, T. Montenay-Garestier and C. Hélène, *J. Biomol. Struct. Dyn.*, 1991, **9**, 411.
37 J.-L. Mergny, J.-S. Sun, M. Rougée, T. Montenay-Garestier, F. Barcelo, J. Chomilier and C. Hélène, *Biochemistry*, 1991, **30**, 9791.
38 D. A. Rusling, T. Brown and K. R. Fox, *Biophys. J.*, 2006, **123**, 134.
39 N. Svanvik, J. Nygren, G. Westman and M. Kubista, *J. Am. Chem. Soc.*, 2001, **123**, 803.
40 E. Privat, T. Melvin, U. Asseline and P. Vigny, *Photochem. Photobiol.*, 2001, **74**, 532.
41 E. Privat, T. Melvin, F. Merola, G. Schweizer, S. Prodhomme, U. Asseline and P. Vigny, *Photochem. Photobiol.*, 2002, **75**, 201.
42 C. R. Cantor, M. M. Warshaw and H. Shapiro, *Biopolymers*, 1970, **9**, 1059.
43 Y. Aubert, S. Bourgerie, L. Meunier, R. Mayer, A.-C. Roche, M. Monsigny, N. T. Thuong and U. Asseline, *Nucleic Acids Res.*, 2000, **28**, 818.